Evaluating visibility of age spot and freckle based on simulated spectral reflectance distribution and facial color image

Misa Hirose,[a] Saori Toyota,[a] Norimichi Tsumura[a]
[a]Chiba University, Graduate School of Advanced Integration Science, 1-33 Yayoi-cho, Chiba, 263-8522, Japan

Abstract. In this research, we evaluate the visibility of age spot and freckle with changing the blood volume based on simulated spectral reflectance distribution and the actual facial color images and compare these results. First, we generate three type of spatial distribution of age spot and freckle in patch like images based on the simulated spectral reflectance. The spectral reflectance is simulated by using Monte Carlo simulation of light transport in multi-layered tissue. Next, we reconstruct the facial color image with changing the blood volume. We acquire the concentration distribution of melanin, hemoglobin and shading components by applying the independent component analysis on a facial color image. We reproduce images by using the obtained melanin and shading concentration and the changed hemoglobin concentration. Finally, we evaluate the visibility of pigmentations using simulated spectral reflectance distribution and facial color images. In the result of simulated spectral reflectance distribution, we found that the visibility became lower as the blood volume increases. However, we can see that a specific blood volume reduce the visibility of the actual pigmentations from the result of the facial color images.

Keywords: visibility, age spot, freckle, facial color image, subjective evaluation, Monte Carlo simulation

Address all correspondence to: Misa Hirose, Chiba University, Graduate School of Advanced Integration Science, 1-33 Yayoi-cho, Chiba, 263-8522, Japan; Tel: +81-43-290-3262; E-mail:m2s.p.n.s@gmail.com

1 Introduction

Skin is an organ that covers human body and affected by UV irradiation and aging. Age spot and freckle on human skin is caused by these affects. Since human face and skin receive a lot of attention in the human body, appearances of age and the health condition are caused by these pigmentations. Therefore, various studies to reduce the visibility of these pigmentations are performed in cosmetology and medical science.

Skin is a multi-layered tissue consists of epidermis, dermis and subcutaneous mainly. Skin color is determined by pigments such as melanin in the epidermis and hemoglobin in vessels of the dermis. Pigments such as β - carotene and bilirubin are also contained in the skin and make the skin color yellowish. It is known that age spot and freckle are the region where melanin in

epidermis is excessively generated and also the region where the color of these pigmentation is darker than normal skin.

Lihong Wang and Steven L. Jaques produced a standard C-code for Monte Carlo simulation of light transport in multi-layered tissue (MCML) [1]. MCML is a technique for analyzing the color of the skin from the concentration of pigments by simulating photon propagation in multi-layered tissue. Skin color is primarily due to the presence of melanin and hemoglobin pigmentation. Tsumura et al.[2] proposed a method that can extract the melanin and hemoglobin pigmentation from a single image; their method uses independent component analysis and is not affected by changes in the light source or the characteristics of the camera. The detail of this method is described in the Reference 2. We can obtain the concentration distribution of pigments such as melanin and hemoglobin from skin image by this method. We can mutually analyze skin color and the concentration of pigments based on these methods. However, the relation is not well understood between the visibility and amount of pigmentations. If the relation is indicated, the result can be applied to basic cosmetic. In the cosmetics industry, basic cosmetics that promote blood volume have been developed and actually sold. Most consumers discontinue use because basic cosmetics are difficult to see an effectiveness unless they continue to use the cosmetic for a long time. In our research, if the result can be obtained that the promotion of blood volume reduces the visibility of spots and freckles, it is possible to add an immediate value of decrease the visibility to basic cosmetics. Therefore, the result improve consumer motivation and promote continuous use of cosmetics.

In this research, therefore, we evaluated the visibility of age spot with changing the blood volume by using simulated spectral reflectance and facial color images and compare these results. In the section 2, we generated age spot and freckle distribution in patch like images form

simulated spectral reflectance by using MCML with changing the melanin and blood volume. We made three type of spatial distributions of age spot and freckle in patch like images. In section 3, the facial color image with changing blood volume is made by using various concentration of hemoglobin, where we acquired the concentration by applying independent component analysis on the image. In section 4, finally, we perform subjective evaluation for the visibility of the age spot and freckle distribution in patch like images generated from simulated spectral reflectance in section 2 and the facial color images in section 3.

2 Theory: Generating Age Spot and Freckle Distribution in Patch like Images from Simulated Spectral Reflectance based of Monte Carlo Simulation for Photon Migration

2.1 Monte Carlo Simulation for Photon Migration

Our research utilized Monte Carlo simulation of light transport in multi-layered tissue (MCML) to simulate the spectral reflectance of normal skin, age spot and freckle. MCML is constituted by following the propagation of photons in tissue as shown in Fig.1.

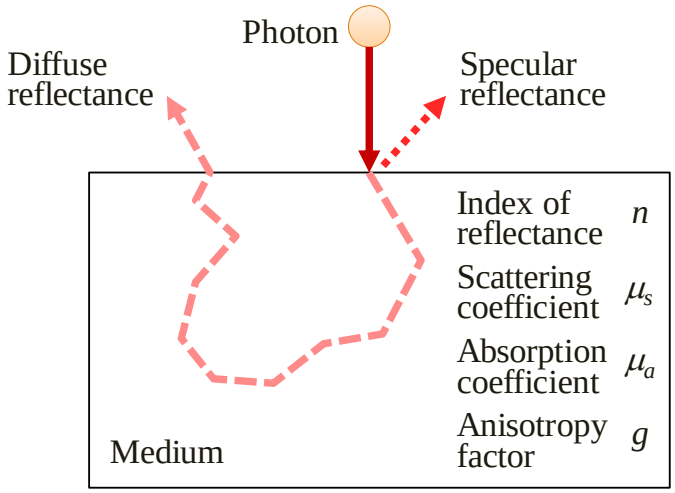

Fig. 1 The movement of photon through a medium calculated by Monte Carlo simulation

2.2 Four-Layered Model for Human Skin

We generate four-layered skin model composed of stratum corneum, epidermis, papillary dermis and reticular dermis to simulate the spectral reflectance by MCML [3]. Figure 2 shows the skin model. We set the thickness *t*, index of refraction *n*, scattering coefficient μ_s, anisotropy factor *g* and absorption coefficient μ_a for each layer [4]. The scattering coefficient μ_s and anisotropy factor *g* are the same value for each layer and shown in Fig.3(a). Anisotropy factor *g* is approximated from experimentally measured values as follows.

$$g = 0.62 \times (0.92 \times 10^{3})\lambda, \tag{4}$$

where λ is the wavelength of light in nanometers. The absorption coefficient μ_a is defined by the absorption coefficient and concentration of pigments. In this research, we consider six kinds of pigments, eumelanin and pheomelanin in the epidermis, oxyhemoglobin, deoxyhemoglobin and bilirubin in the papillary dermis and reticular dermis and β-carotene in all layer. The absorption coefficients of eumelanin $\mu_{a.eu}$ and pheomelanin $\mu_{a.pheo}$ are shown in Fig.3(b). These absorption coefficients are approximated from experimentally measured values as follows in the Reference 5.

$$\begin{aligned} \mu_{a.eu} &= 6.6 \times 10^{11} \times \lambda^{-3.33} \\ \mu_{a.pheo} &= 2.9 \times 10^{15} \times \lambda^{-4.75}, \end{aligned} \tag{5}$$

where the absorption coefficients of oxyhemoglobin, deoxyhemoglobin, β-carotene and bilirubin are calculated by using the experimentally measured molar extinction coefficients shown in Fig.3(c), (d) as follows [4,6].

$$\mu_{a.ohb} = 2.303 \times S \times \frac{\varepsilon_{ohb}}{66500} c_{hb}$$
$$\mu_{a.car} = 2.303 \times \frac{\varepsilon_{car}}{537} c_{car} \tag{6}$$
$$\mu_{a.bil} = 2.303 \times \frac{\varepsilon_{bil}}{585} c_{bil},$$

where ε_{ohb}, ε_{car} and ε_{bil} are the molar extinction coefficients, $\mu_{a.ohb}$, $\mu_{a.car}$ and $\mu_{a.bil}$ are the absorption coefficients, c_{hb}, c_{car} and c_{bil} are the concentration, 66500, 537 and 585 are molecular weight, and S is oxygen saturation. The subscript *hb*, *ohb*, *car* and *bil* indicate hemoglobin, oxyhemoglobin, β-carotene and bilirubin. The absorption coefficient of deoxyhemoglobin μ_{dhb} is computed by replacing ε_{ohb}, S for ε_{dhb}, $(1-S)$ in Eq.6. The concentration of hemoglobin c_{hb} is typically 150[g/L].

The absorption coefficients for each layer $\mu_{a.sc}$, $\mu_{a.epi}$ and $\mu_{a.der}$ are computed as follows [3]. The subscript *sc* and *epi* indicate stratum corneum and epidermis respectively. The subscript *der* indicates both papillary and reticular dermis.

$$\begin{aligned}
\mu_{a.sc} &= \mu_{a.base} + \mu_{a.cs} \\
\mu_{a.epi} &= (M_{eu}\mu_{a.eu} + M_{pheo}\mu_{a.pheo})M + (\mu_{a.base} + \mu_{a.ce})(1 - M) \\
\mu_{a.der} &= (\mu_{a.ohb} + \mu_{a.dhb} + \mu_{a.cd} + \mu_{a.bil})B + (\mu_{a.base} + \mu_{a.ce})(1 - B),
\end{aligned} \tag{7}$$

where $\mu_{a.base}$ is the absorption coefficient of baseline skin such as organelles, cell membranes and fibrils, $\mu_{a.cs}$, $\mu_{a.ce}$ and $\mu_{a.cd}$ are the absorption coefficient of carotene in stratum corneum, epidermis and dermis respectively, M is the volume fraction of melanosomes in epidermis, M_{eu} and M_{pheo} are the volume fraction of eumelanin and pheomelanin in melanosomes, B is the volume fraction of whole blood in dermis. The absorption coefficient $\mu_{a.cs}$, $\mu_{a.ce}$, $\mu_{a.cd}$ and $\mu_{a.base}$ are known parameters and the volume fraction M, M_{eu}, M_{pheo} and B are unknown fraction. The absorption coefficient of baseline skin $\mu_{a.base}$ is approximated as follows [7].

$$\mu_{a.base} = 7.84 \times 10^{8} \times \lambda^{-3.255}. \quad (8)$$

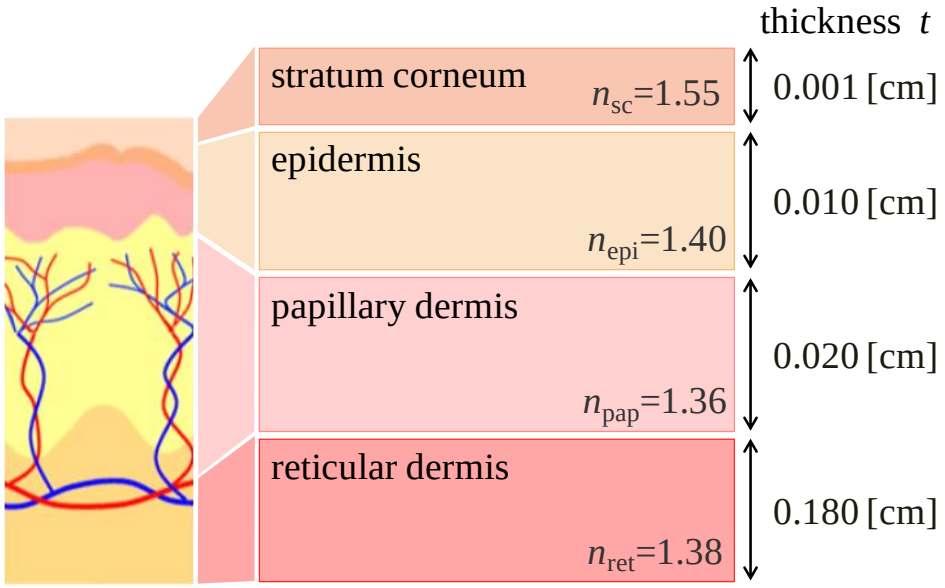

Fig. 2 Four-layered skin model

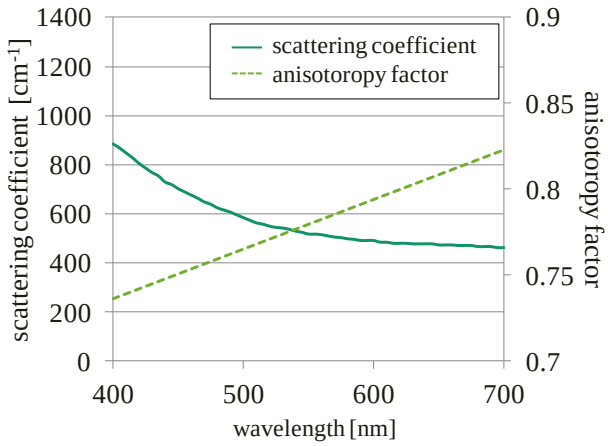

(a)

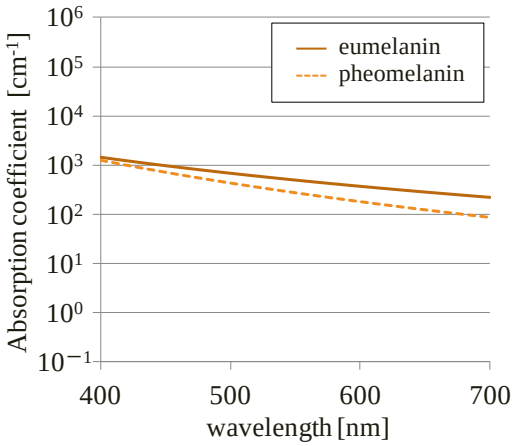

(b)

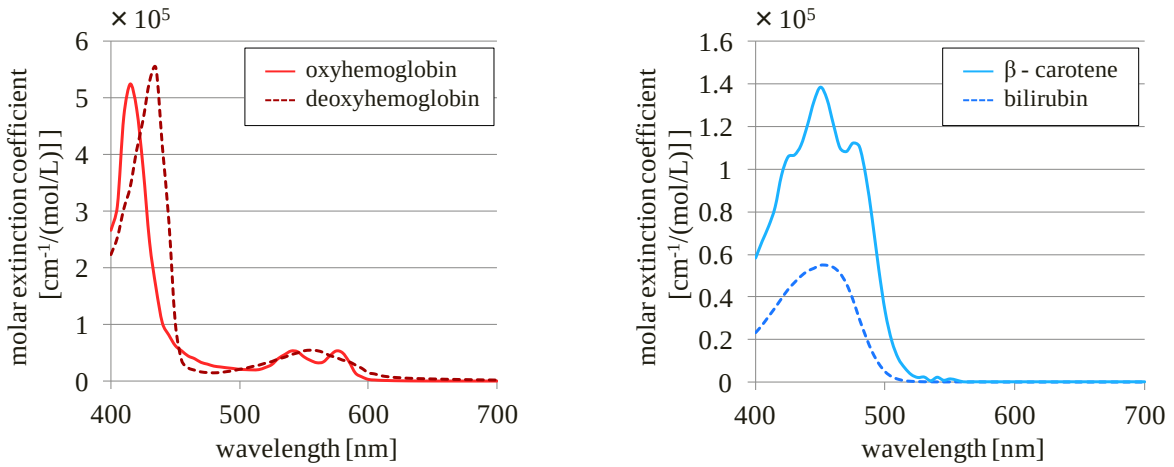

Fig. 3 Optical parameters for MCML : (a) scattering coefficient and anisotropy factor, (b) absorption coefficient of eumelanin and pheomelanin, (c) molar extinction coefficients of β - carotene and bilirubin and (d) molar extinction coefficients for oxyhemoglobin and deoxyhemoglobin.

2.3 The Concentration of Pigments for Skin, Age Spot and Freckle

We determined the concentration of pigments for normal skin, age spot and freckle to calculate spectral reflectance by MCML. The concentration of pigments for normal skin was determined such that simulated spectral reflectance approaches the average of measured spectral reflectance for 59 Japanese women. The oxygen saturation S was 75%, the concentration of β-carotene c_{car} and bilirubin c_{bil} were indicated in Table 1 [8]. Therefore, we empirically determined the volume fraction of melanosomes M, eumelanin M_{eu}, pheomelanin M_{pheo} and whole blood B from the average spectral reflectance.

The measured spectral reflectance and the result of simulation by MCML are shown in Fig.4, where the volume fraction of melanosomes was epidermis M is 3.0%, the volume fraction of eumelanin M_{eu} and pheomelanin M_{pheo} in melanosomes were 10.0% and 90.0% respectively and the volume fraction of whole blood in dermis B was 3.0%. The color difference ΔE between

measured and simulated spectral reflectance was 0.923 in CIELAB color space. It is known that we cannot perceive the difference between two colors if the value of ΔE is less than from 1 to 3 [9]. Thus, the result of simulation is close to the measured spectral reflectance.

We set the volume fraction of melanosomes M for age spot and freckle more than that for normal skin 3.0%, because age spot and freckle are the regions where melanin is excessively generated in epidermis. In this research, we set the volume fraction of melanosomes M for age spot and freckle to 4.0, 5.0 and 6.0%. For computing spectral reflectance with changing blood volume, we increased the blood volume for skin, age spot and freckle from 3.0% to 20.0%.

Table 1 The concentration of β - carotene and bilirubin for each layer

	β - carotene [g/L]	**Bilirubin [g/L]**
Stratum corneum	22.2×10^{-4}	—
Epidermis	22.2×10^{-4}	—
Papillary dermis	7.00×10^{-4}	7.00×10^{-3}
Reticular dermis	7.75×10^{-4}	7.00×10^{-3}

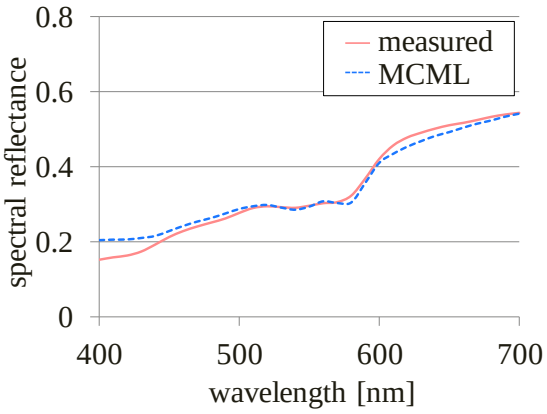

Fig. 4 Measured spectral reflectance and the result of simulation

2.4 Generating Age Spot and Freckle Distribution

We generated age spot and freckle distribution in patch like images from spectral reflectance computed by MCML. First, we converted the spectral reflectance to XYZ color system as follows.

$$
\begin{aligned}
X &= k\int_{400}^{700} R(\lambda)P(\lambda)\bar{x}(\lambda)d\lambda \\
Y &= k\int_{400}^{700} R(\lambda)P(\lambda)\bar{y}(\lambda)d\lambda \\
Z &= k\int_{400}^{700} R(\lambda)P(\lambda)\bar{z}(\lambda)d\lambda \\
k &= 1/\int_{400}^{700} P(\lambda)\bar{y}(\lambda)d\lambda,
\end{aligned}
\tag{9}
$$

where $R(\lambda)$ is spectral reflectance of skin, age spot and freckle, $P(\lambda)$ is spectral distribution of the light source and $x(\lambda)$, $y(\lambda)$, $z(\lambda)$ are color-matching function with a 2° view as the observation condition [10]. The spectral distribution of light source $P(\lambda)$ is 1.0 at all wavelength. Next, we convert these to sRGB. Because, in the subjective evaluation experiment, the conditions of monitor display is sRGB reference viewing environment.

We performed gamma correction with $\gamma = 2.4$ based on the gamma characteristics of display. As shown Fig.5, we generated 3 kinds of spatial distribution. The terms “without split”, “9-split” and “random” indicate one large age spot, nine little age spot and freckle, respectively. The size of images is 500×500 (250,000 pixel), and age spot and freckle is 14,400 pixel. We applied a Gaussian filter to blur the boundary of skin and age spot. The Gaussian filter was defined by the kernel size and sigma σ. We set the kernel size 10×10 and $\sigma = 10$.

(a) (b) (c)

Fig. 5 Distribution of age spot and freckle in patch like images : (a) Without split, (b) 9-split nad (c) Random

3 Theory: Generating Skin Color Image with Changing Blood Volume based on Independent Component Analysis

3.1 Independent Component Analysis of Skin Color Image

We use the independent component analysis of skin color image proposed by Tsumura *et al.* to reproduce the color of real skin, age spot and freckle on the face with changing blood volume. As shown in Fig.6, we can acquire the concentration distribution of shading, melanin and hemoglobin using this technique [2,12,13]. We will describe this approach in this section.

Figure 7 is the skin model consists of epidermis and dermis. The skin color is denoted by melanin in the epidermis and hemoglobin in the dermis mainly. The light incident on the skin is separated into specular reflectance and diffuse reflectance. The specular reflectance indicates light source color, the diffuse reflectance indicates skin color. In this research, we consider the diffuse reflectance as observed signal and take the diffuse reflectance image of face based on a method proposed by Ojima *et al.* [11]. The specular reflectance is removed by setting the polarizing filter orthogonally in front of camera and light source.

We show the relation of the skin model and the RGB value of the facial image. If we assume that Modified Lambert-Beer is satisfied, the diffuse reflectance of skin is shown as follows.

$$L(x, y, \lambda) = e^{-\rho_m(x,y)\sigma_m(\lambda)l_e(\lambda)-\rho_h(x,y)\sigma_h(\lambda)l_d(\lambda)} E(x, y, \lambda) \tag{11}$$

where $L(x, y, \lambda)$, $E(x, y, \lambda)$ are the spectral irradiance at (x, y) of the reflected and incident light, $\rho_m(x, y)$, $\rho_h(x, y)$ are the concentration of melanin and hemoglobin, $\sigma_m(x, y)$, $\sigma_h(x, y)$ are the absorption cross-section of melanin and hemoglobin, and $l_e(\lambda)$, $l_d(\lambda)$ are optical path length of light passing through the epidermis and dermis. Sensor response of a digital camera as the observed signal $v_i(x, y)$ is expressed as follows.

$$v_i(x,y) = k\int e^{-\rho_m(x,y)\sigma_m(\lambda)l_e(\lambda)-\rho_h(x,y)\sigma_h(\lambda)l_d(\lambda)} E(x,y,\lambda)s_i(\lambda)d\lambda \tag{12}$$

where k, $s_i(\lambda)$ are the gain and spectral sensitivity of the digital camera, and $i = (R, G, B)$. The spectral sensitivity of the camera $s_i(\lambda)$ is approximated as $\delta_i(\lambda)$ in a narrow frequency band by the assumption as shown in Ref.2. In addition, we assume that the lighting environment is distand and that its spectrum does not vary with direction, so that the irradiance can be written as $E(x,y,\lambda) = p(x,y)\overline{E}(\lambda)$, where $p(x,y)$ encodes shape-induced shading variation. Thus, Eq.12 is rewritten by Eq.13.

$$v_i(x,y) = ke^{-\rho_m(x,y)\sigma_m(\lambda)l_e(\lambda)-\rho_h(x,y)\sigma_h(\lambda)l_d(\lambda)} p(x,y)\overline{E}(\lambda_i) \tag{13}$$

We convert the RGB color space to the optical density space as follows.

$$\boldsymbol{v}^{\boldsymbol{log}}(x,y) = \rho_m(x,y)\boldsymbol{\sigma_m}(\lambda) - \rho_h(x,y)\boldsymbol{\sigma_h}(\lambda) + p^{\log}(x,y)\boldsymbol{1} + \boldsymbol{e}^{\boldsymbol{log}} \tag{14}$$

where

$$\begin{aligned}
\boldsymbol{v}^{\boldsymbol{log}}(x,y) &= [\log(v_R(x,y)),\log(v_G(x,y)),\log(v_B(x,y))]^T \\
\boldsymbol{\sigma_m} &= [\sigma_m(\lambda_R)l_e(\lambda_R),\sigma_m(\lambda_G)l_e(\lambda_G),\sigma_m(\lambda_B)l_e(\lambda_B)]^T \\
\boldsymbol{\sigma_h} &= [\sigma_h(\lambda_R)l_d(\lambda_R),\sigma_h(\lambda_G)l_d(\lambda_G),\sigma_h(\lambda_B)l_d(\lambda_B)]^T \\
\boldsymbol{1} &= [1,1,1]^T \\
\boldsymbol{e}^{\boldsymbol{log}} &= [\log(E(\lambda_R)),\log(E(\lambda_G)),\log(E(\lambda_B))]^T \\
p^{\log}(x,y) &= \log(p(x,y)) + \log(k)
\end{aligned} \tag{15}$$

The observed signal $\boldsymbol{v}^{\boldsymbol{log}}$ is expressed by the bias vector $\boldsymbol{e}^{\boldsymbol{log}}$ and the weighted linear combination of $\boldsymbol{\sigma_m}$, $\boldsymbol{\sigma_h}$ and $\boldsymbol{1}$. The relation of observed signal and three independent signals is shown in Fig.8. The skin color is distributed on a two-dimensional plane consists of the vector of melanin and hemoglobin component. These vectors are obtained by performing an independent component analysis on the observed signal. We remove the shading information by projecting the skin color vector on the two-dimensional plane along the shading vector, and acquire the concentration of melanin and hemoglobin by projecting onto melanin and hemoglobin vectors.

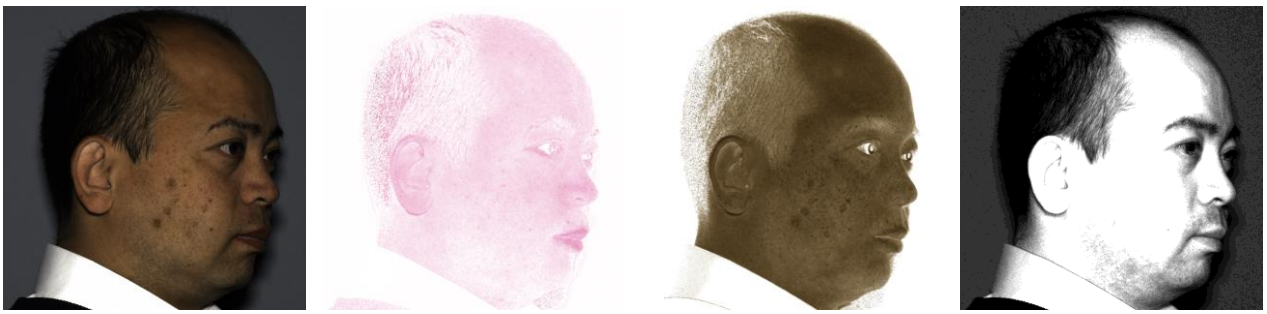

(a) (b) (c) (d)

Fig. 6 The result of applying the independent component analysis on the facial color image : (a) original image, (b) hemoglobin, (c) melanin and (d) shading

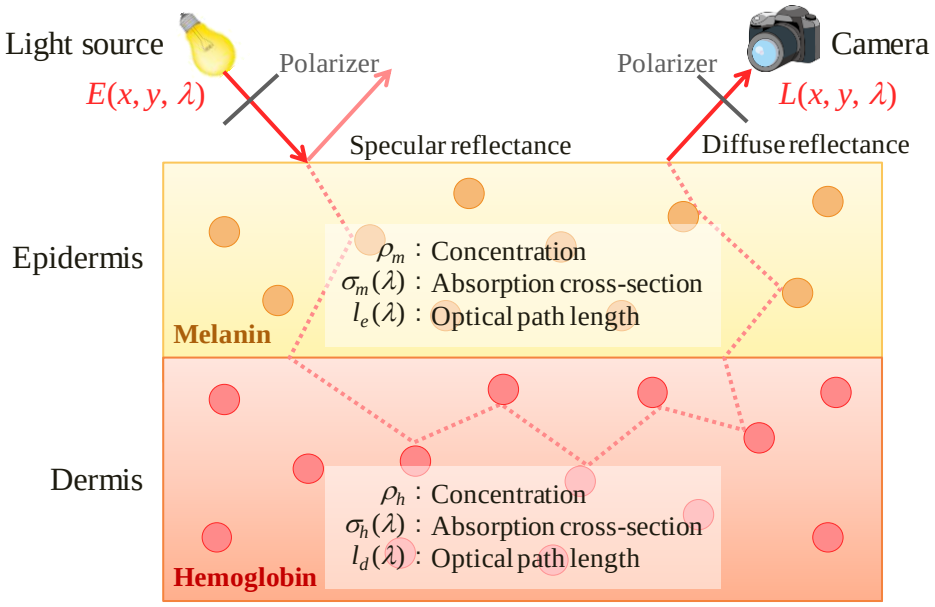

Fig. 7 Two-layered skin model and the movement of photon incident on the skin

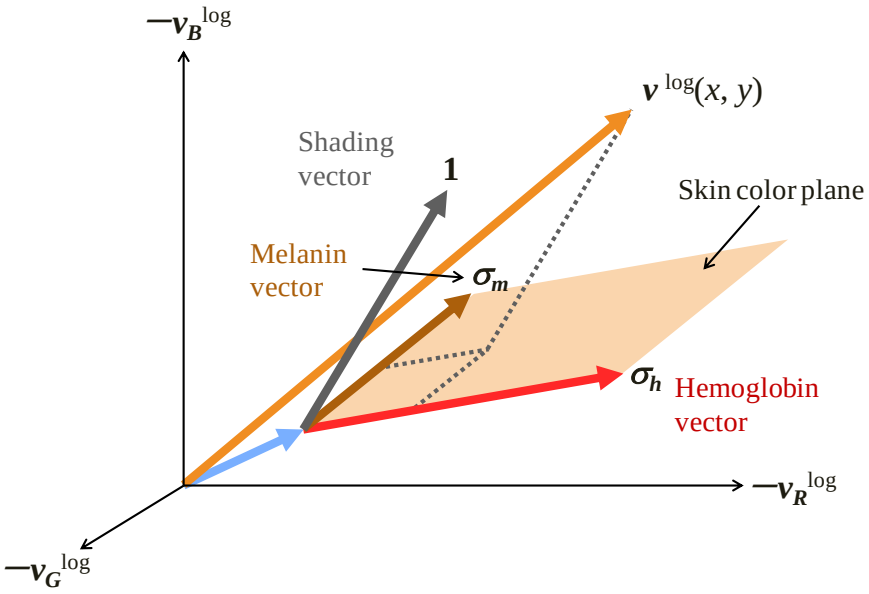

Fig. 8 Relationship of independent signals and three observation signal in the skin model

3.2 Generating Skin Color Image with Changing Blood Volume

In this section, we show the process of generating skin color image with changing blood. First, we acquire the concentration distribution of shading, melanin and hemoglobin by the independent component analysis. We change the concentration of hemoglobin from −5% to + 20%. We reconstruct the skin color image using these concentrations of pigments. At last, we perform gamma correction based on the gamma characteristics of display.

4 Experiment: Evaluating the Visibility of Pigmentations using Patch like Images and Facial Color Images

4.1 Experimental set-up

Figure 9(a) shows the experimental room covered with black-out curtain. The display is 19 inch LCD and the viewing distance was approximately 87 cm that corresponded with three times the

height of the display. Two images are displayed side-by-side at random on display, and the size of images and the display is shown in Fig.9(b).

4.2 Subjective experiment

In the subjective evaluation, we utilized the method of paired comparison. Observers select an image that age spot and freckle in patch like images is less noticeable. We evaluated the results by Thurstone's case V scaling. In the subjective evaluation of the pigmentation distribution and facial color images, the numbers of observers are 10 and 12 respectively.

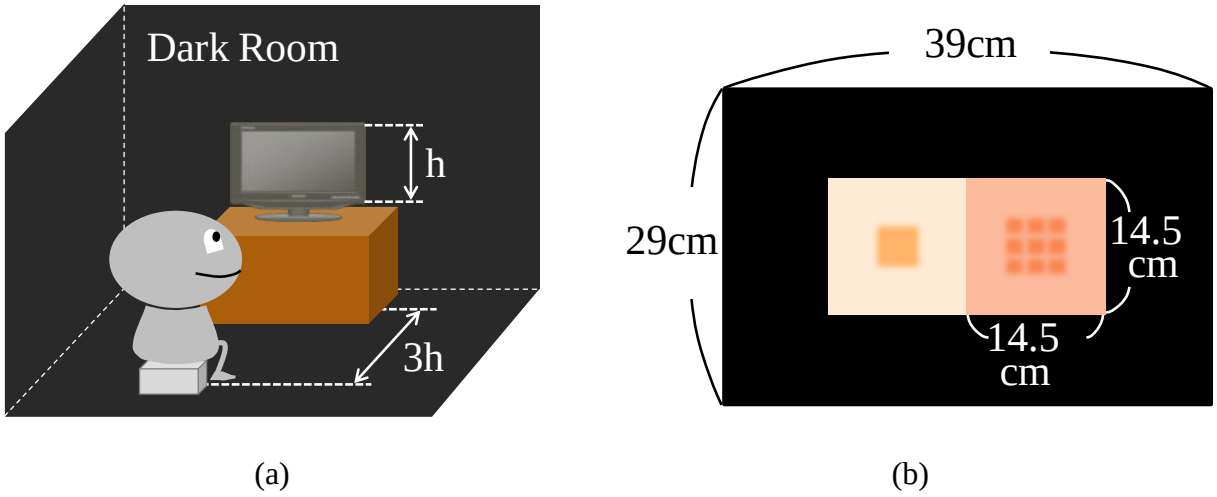

(a) (b)

Fig. 9 Experiment environment : (a) experimental room and (b) size of display and patch like images

4.3 Results and Discussion

Figure 10 shows 27 images of age spot and freckle distribution in patch like images generated from spectral reflectance simulated by MCML. The melanin volume of age spot and freckle are 4.0, 5.0 and 6.0%, and the blood volume of skin, age spot and freckle are 3.0, 10.0 and 20.0%. There are 3 types of the spatial distribution of age spot and freckle, that is without split, 9-split, and random. Figure 11 shows the result of subjective evaluation for the images shown in Fig.10.

The vertical axis indicates the visibility of age spot and freckle in patch like images. This value becomes larger as the visibility of the pigmentations increases. The horizontal axis is the image numbers corresponding to those in Fig.10. The color of the bar chart indicates the blood volume of skin, age spot and freckle. From the results, we could see that the age spot and freckle in patch like images become less noticeable, regardless of the spatial distribution and melanin volume of those, as the blood volume increases. We focused on the effect of increasing the blood volume on the reduction of visibility when the melanin volume is 4.0% and 6.0%. If the spatial distribution is "without split", the effect is larger compared to "random" when the melanin volume is 4.0%. When the melanin volume is 6.0%, the effect is opposite to the above. If we want to reduce the visibility of age spot and freckle in patch like images, therefore, the increase of the blood volume is effective in the case of "without split" when the amount of these pigments is low. In contrast, the increase of the blood volume is effective in the case of "random" when the color of these pigments is dark.

Figure 12 shows 6 images of facial image with the change of the blood volume and Fig.13 shows the result of subjective evaluation for images shown in Fig.12. The left vertical axis indicates the same evaluated value as Fig.11, and this value becomes larger as the visibility of the pigmentations increases. The right vertical axis indicates the color difference of pigmentations and skin. The color difference is computed by using the average color of the region of skin and pigmentations. The horizontal axis is the image numbers corresponding to those in Fig.12. From Fig.13, we can see that the visibility of age spot and freckle is the lowest in the case of the amount of change in blood volume +5%. However, the color difference of pigmentations and skin is smaller as the blood volume increases. We think that perception of the

color difference became difficult because the color of the actual skin is non-uniform unlike the images of age spot and freckle distribution generated by MCML.

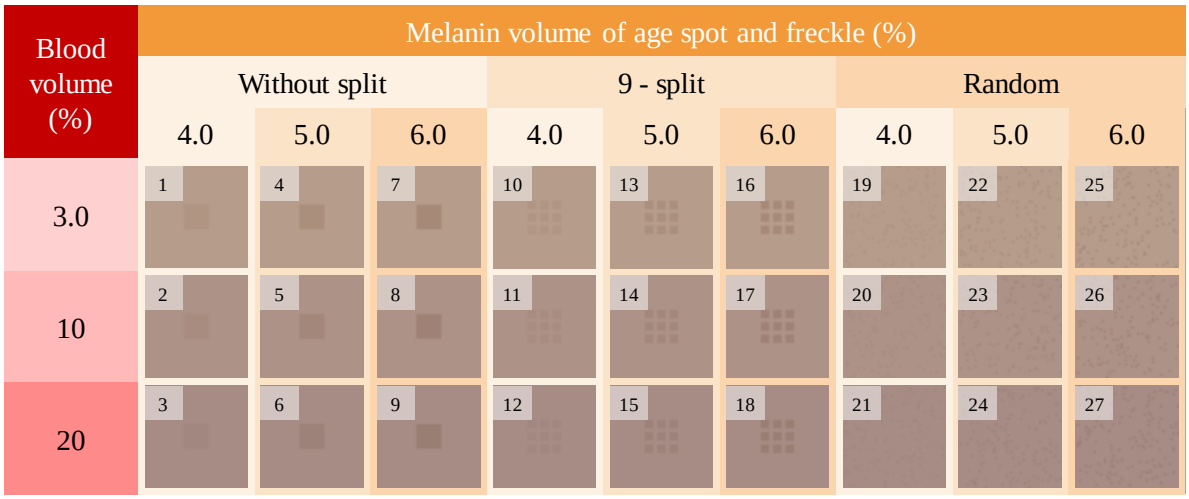

Fig. 10 Generated images of age spot and freckle distribution in patch like images

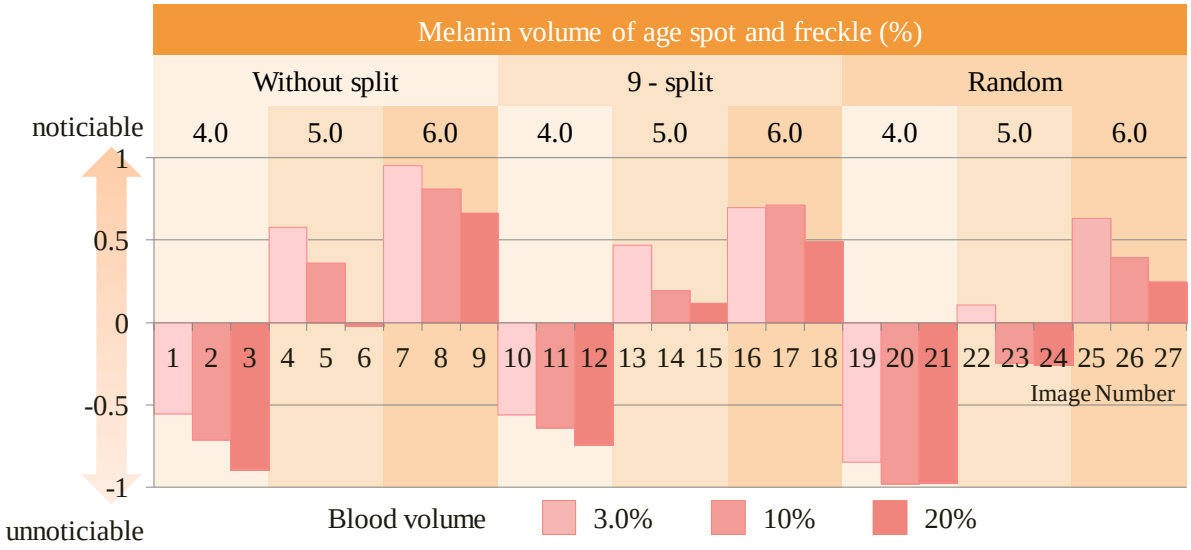

Fig. 11 Result of subjective evaluation for age spot and freckle distribution in patch like images

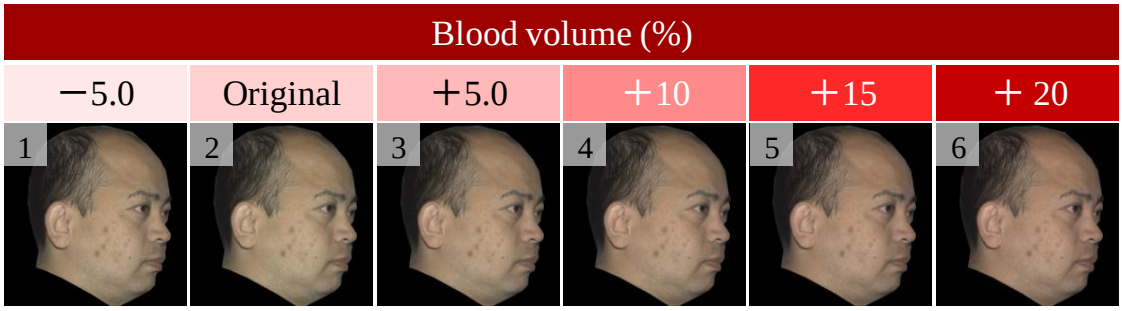

Fig. 12 Facial color images with changing blood volume

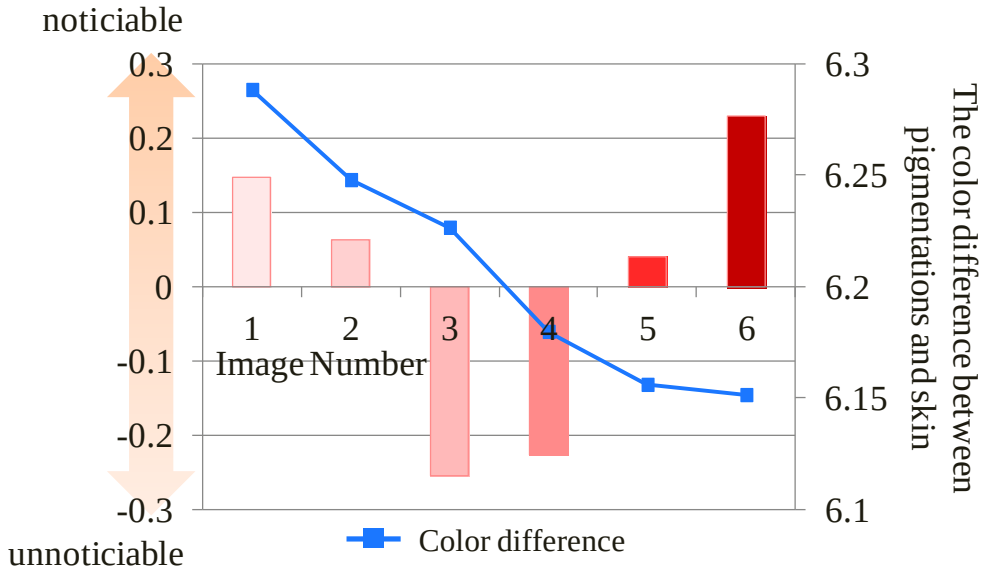

Fig. 13 Result of subjective evaluation for the facial color images and the color difference of pigmentations and skin

5 Conclusion and discussion

In this research, we evaluate the visibility of age spot and freckle with changing blood volume based on patch like images and facial color images, and compare these results. The result of evaluating the pigmentation distribution in patch like images indicated that the visibility becomes lower as the blood volume increases. We could also see that the effect of increasing the blood volume on the reduction of visibility varies depending on the melanin volume and spatial

distribution of these pigmentations. Since the color of pigmentation area is also changed by increasing blood volume, we didn't know whether the visibility is changed by increasing blood volume. In our results, we found that the promotion of blood volume decrease the visibility . To apply to basic cosmetics, we think that it is necessary to examine how much blood volume can be increased by cosmetic products. However, the result of evaluating the actual facial color images shows that a specific blood volume reduce the visibility of age spot and freckle. Because the color of the skin, age spot and freckle is actually non-uniform and different from the patch like images generated by simulated spectral reflectance. Therefore, it is necessary to find a specific blood volume to reduce the visibility of the actual pigmentations. In the future work, we investigate the effect of the color unevenness of skin, age spot and freckle.

In this paper, we performed the experiment using just one male facial image. If we perfume lots of experiments for various additional facial images with the change of gender, age, race, shape, skin type and so on, we may obtain the complicated results since the visibility of age spot and freckle will be affected by the many attributes on face. From this reason we limited our experiments only to show the difference of evaluation results between patch like image and facial color image.

Acknowledgments

This research is partly supported by JSPS Grants-in-Aid for Scientific Research (24560040)

References

1. Wang L. and Jacques S. L., "Monte Carlo Modeling of Light Transport in Multi-layered Tissues in Standard C", University of Texas M. D. Anderson Cancer Center (1992).

2. N. Tsumura, N. Ojima, K. Sato, *et al.*, “Image-based skin color and texture analysis/synthesis by extracting hemoglobin and melanin information if the skin”, ACM Transactions on Graphics, Vol.22, No.3, 770-779 (2003).
3. Aravind Krishnaswamy and Gladimir V.G. Baranoski, “A Biophysically-Based Spectral Model of Light Interaction with Human Skin”, EUROGRAPHICS, Vol.23, No.3, pg.331-340 (2004)
4. N. Tsumura, M. Kawabuchi, H. Haneishi and Y. Miyake, “Mapping pigmentation in human skin from multi-channel visible spectrum image by inverse optical scattering technique”, Journal of Imaging Science and Technology, Vol.45, No.5, pg.444-450 (2000).
5. Donner, C. and Jensen, H.W., “A Spectral BSSRDF for Shading Human Skin”, EUROGRAPHICS, pg.409-417 (2006).
6. Oregon Medical Laser Center, http://omlc.ogi.edu/.
7. Jacques S. L., “Skin Optics”, Organ Medical Center News, http://omlc.ogi.edu/news/jan98/skinoptics.html (1998).
8. Anders Vahlquist, M.D. et al. “Vitamin A in Human Skin: II Concentrations of Carotene, Retinol and Dehydroretinol in Various Compornents of Normal Skin”, Journal of Investigative Dermatology, Vol.79, No.2, pg.94-97 (1982).
9. R. W. G. Hunt, “Measuring Color” (1998).
10. Colour Matching Functions, http://cvrl.ioo.ucl.ac.uk/cmfs.htm.
11. N. Ojima, T. Minami and M. Kawai, “Transmittance measurement of cosmetic layer applied on skin by using processing”, Proceeding of The 3rd Scientific Conference of the Asian Societies of Cosmetic Scientists, vol.114 (1997).
12. Saori Toyota, Izumi Fujiwara, Misa Hirose, Nobitoshi Ojima, Ogawa-Ochiai Keiko, Norimichi Tsumura, “Principal Component Analysis for the Whole Facial Image With Pigmentation Separation and Application to the Prediction of Facial Images at Various Ages”, Journal of Imaging Science and Technology, Vol.58, No.2,020503-1-020503-11,Mar.-Apr,(2014)

13. Yuri Tatsuzawa, Misa Hirose, Nobutoshi Ojima, Keiko Ogawa-Ochiai and Norimichi Tsumura, "Analyzing the Individual Relationship between Habit of UV Protection and Melanin Pigmentation based on the Change of Facial Images for 7 Years", Color and Imaging Conference, Darmstadt, Germany, Proceedings pp.24-28, (2015)
14. L.G. Henyey, J.L. Greenstein, Diffuse radiation in the galaxy, Astrophysical Journal 93:70-83, 1941.

Caption List

Fig. 1 The movement of photon through a medium calculated by Monte Carlo simulation

Fig. 2 Four-layered skin model

Fig. 3 Optical parameters for MCML : (a) scattering coefficient and anisotropy factor, (b) absorption coefficient of eumelanin and pheomelanin, (c) molar extinction coefficients of β -carotene and bilirubin and (d) molar extinction coefficients for oxyhemoglobin and deoxyhemoglobin.

Fig. 4 Measured spectral reflectance and the result of simulation

Fig. 5 Distribution of age spot and freckle : (a) Without split, (b) 9-split nad (c) Random

Fig. 6 The result of applying the independent component analysis on the facial color image : (a) original image, (b) hemoglobin, (c) melanin and (d) shading

Fig. 7 Two-layered skin model and the movement of photon incident on the skin

Fig. 8 Relationship of independent signal and three observation signal in the skin model

Fig. 9 Experiment environment : (a) experimental room and (b) size of display and images

Fig. 10 Generated images of age spot and freckle distribution

Fig. 11 Result of subjective evaluation for age spot and freckle distribution

Fig. 12 Facial color images with changing blood volume

Fig. 13 Result of subjective evaluation for the facial color images and the color difference of pigmentations and skin

Table 1 The concentration of β-carotene and bilirubin for each layer